Chapter 6

Design of Weld Metal Avoiding Post–Weld Heat Treatment

Low–carbon creep–resisting steels used in the construction of power plant or in the petrochemical industry generally contain chromium, molybdenum, niobium or vanadium as the significant alloying additions. These elements either provide oxidation and corrosion protection (for example, chromium) or on tempering they form stable carbides which impede creep deformation. The steels have major applications in the fabrication of pressure vessels, boiler steam pipes, steam generating and handling equipment, high pressure tubes with thick walls, turbine rotors, superheater tubes, coal to methane conversion plants and petrochemical reactors for the treatment of heavy oils and tar sands bitumen [116]. The steels might typically be used within the temperature range 480–600 °C, the service stresses being of the order of 15–40 MPa. The required microstructure is produced by austenitisation followed by tempering at a temperature which is above that encountered during service. A typical tempering heat treatment may therefore involve temperatures in the range 650–750 °C, for some 4–20 h, depending on the detailed chemical composition and also the section size.

Further heat treatments are required following welding operations. The heat introduced during welding has a significant influence on the solid metal in the close proximity of the weld. Microstructures may be created in this heat–affected zone, which are hard (martensitic) and untempered. Furthermore, residual stresses arise from the shrinkage of the weld as it cools from the liquid state. One purpose of a post–weld heat treatment is to ameliorate both of these changes due to welding.

There are many components of a power plant where it is incredibly difficult to introduce post–weld heat treatments, primarily because of the large scale of the plant involved, but also due to the tight packing of components. One such case is the boiler which contains a myriad of pipes, as illustrated in Fig. 6.1. To reduce the costs of implementing post–weld heat treatments in such circumstances, Mitsubishi Heavy Industries in Japan has developed a new steel, designated

HCM2S, which replaces the classical $2\frac{1}{4}$Cr–1Mo alloy [117]. The latter requires post–weld heat treatment whereas the former, due to its lower hardness in all microstructural conditions, does not. The development of the new steel does not entirely resolve the difficulties since the weld metal used to fill the gaps between plates to be joined also requires heat–treatment. The purpose of the work presented in this Chapter was therefore to design, using the methodologies described in earlier Chapters, a welding alloy which itself does not require post–weld heat treatment.

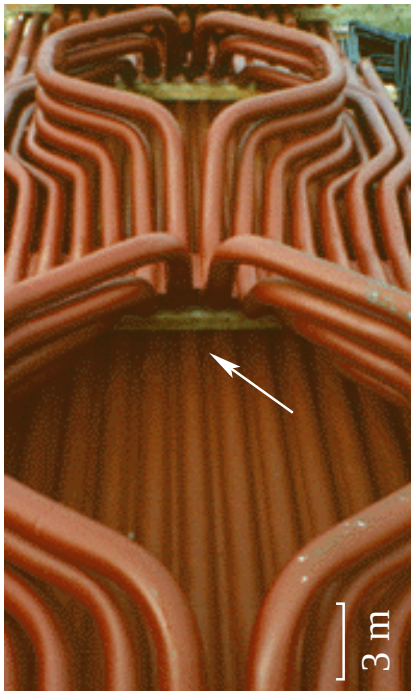

Figure 6.1: Complex shapes of boiler tubes used in power plant. The arrow shows two boiler tubes joined together with a supporting plate.

6.1 Novel Cr–W–V–Nb Steel (HCM2S)

This material was developed in 1993 [118] for the construction of boilers, with the aim of avoiding post–weld heat treatments. This essentially requires a relatively low hardness following an austenitisation treatment of the kind which might occur in the heat–affected zone of a weld, without compromising the creep properties. Conventional $2\frac{1}{4}$Cr–1Mo wt% steel contains a carbon concentration of 0.1 wt% or more; it needs post–weld heat treatment to restore the ductility and decrease the hardness in the heat–affected zone. The hardness of $2\frac{1}{4}$Cr–1Mo steel is attributed mainly to its carbon and molybdenum concentrations, whereas the chromium serves primarily to provide limited oxidation and corrosion resistance. Molybdenum serves to form a carbide which enhances creep strength.

Therefore, the idea behind the new steel HCM2S was to reduce the carbon concentration, to replace molybdenum with tungsten (which remains in solid solution) and to enhance creep strength using small concentrations of niobium and vanadium, both of which are strong carbide formers [119], Table 6.1. The gross microstructure following heat treatment is essentially the same as that of $2\frac{1}{4}$Cr–1Mo, consisting of tempered bainite Fig. 6.2.

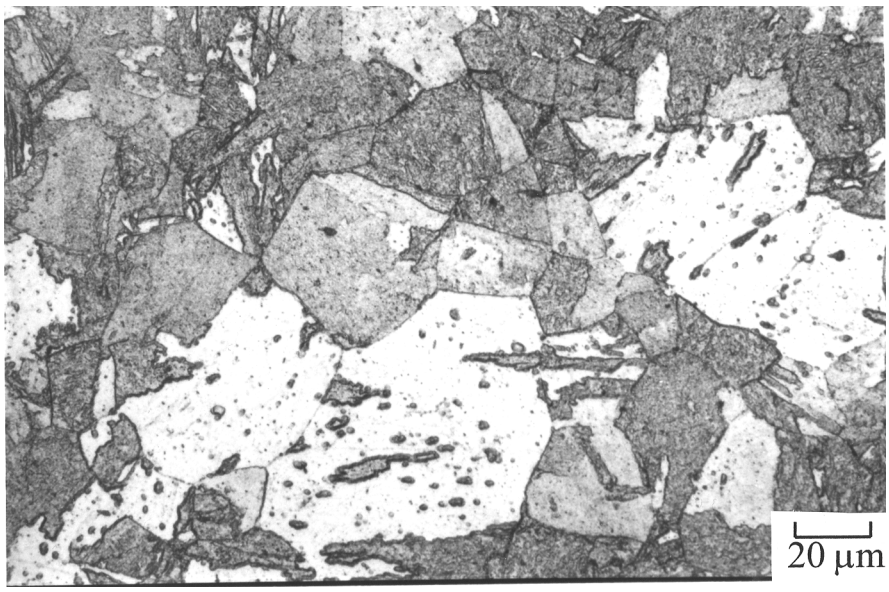

Figure 6.2: Tempered microstructure of as–received HCM2S steel tube. The tube is tempered at 770 °C for 1 hour after air cooling from 1050 °C (1 h). The sample is etched using 2% nital.

The flow chart illustrating the development of HCM2S steel is shown in Fig. 6.3. Due to the lower carbon concentration in HCM2S, the maximum hardness obtained for typical cooling rates is reduced to about 300 HV which is some 50 HV lower than $2\frac{1}{4}$Cr–1Mo steel, Fig. 6.4. Insensitivity to cooling rate at higher cooling rates is desirable in welding. The excellent creep strength of HCM2S is due to the substitution of tungsten for molybdenum, with slight additions of boron together with the precipitation of vanadium and niobium carbide. Here the solid solution strengthening is due to tungsten and the precipitation strengthening due to vanadium and niobium. The addition of boron has the effect of stabilising $M_{23}C_6$ and $M_{23}(C,B)_6$ on grain boundaries, thereby retarding the recrystallisation of grains during service [120]. A comparison of the creep resistance of HCM2S against conventional $2\frac{1}{4}$Cr–1Mo steels is shown in Fig. 6.5. HCM2S has the composition 1.6W-0.1Mo-0.25V-0.05Nb wt% with 0.06 wt% average carbon content.

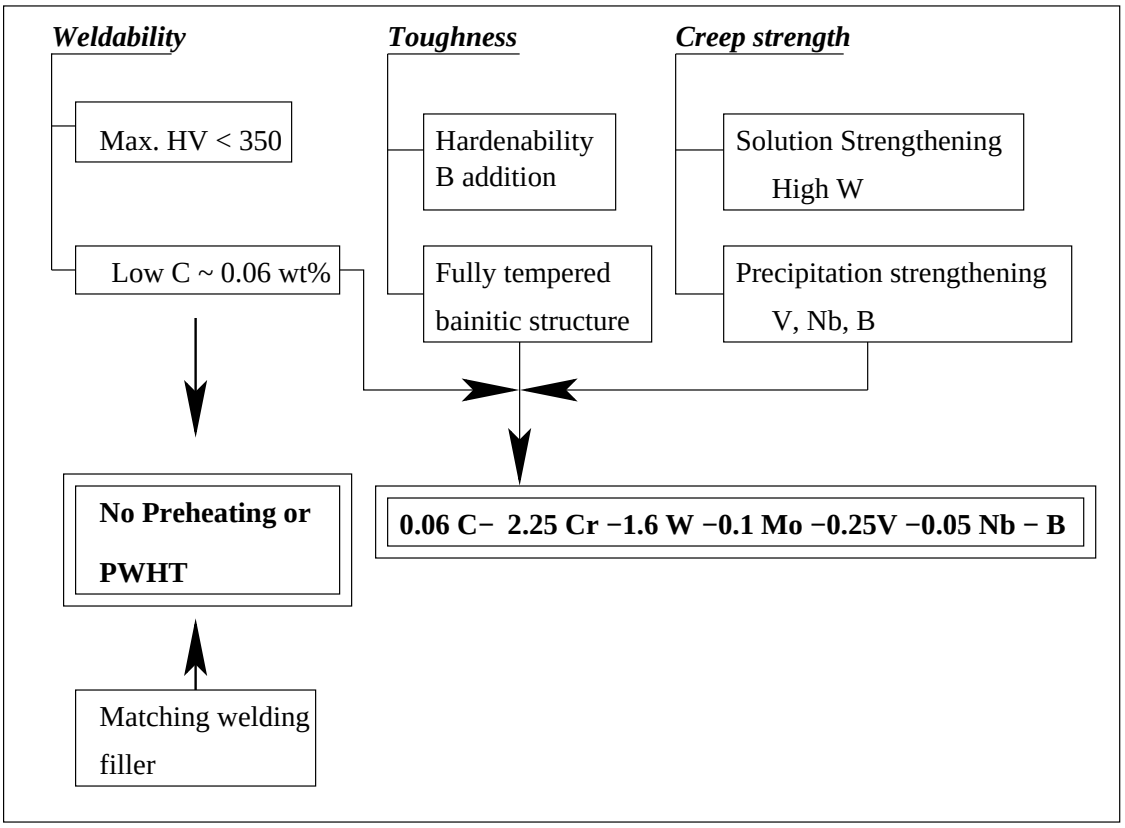

Figure 6.3: Development philosophy of HCM2S steel [117]. PWHT corresponds to post–weld heat treatment.

C	Si	Mn	P	S	Ni	Cr	Mo	W	V	Nb	B	Al	N
0.06	0.20	0.47	0.006	0.002	0.10	2.27	0.09	1.50	0.23	0.05	0.004	0.009	0.008

Table 6.1: Chemical composition (in wt%) of HCM2S base metal [119, 117].

6.1.1 Welding of HCM2S Steel

Some research has already been done at Sumitomo Metal Industries in Japan to attempt the welding of HCM2S steel. Their weld metal chemical compositions are shown in Table 6.2. The heat input used in the gas tungsten arc welding (GTAW) process is 1.85 kJ mm^{-1} and in shielded metal arc welding (SMAW) 1.5 kJ mm^{-1}, with an interpass temperature of 225 °C in each case. The maximum as–welded yield strength (YS) of the weld metal is reported to be 877 MPa (Table 6.3) and the Vickers hardness is stated to be in the range 300 to 350. The weld metals clearly have good mechanical properties and the creep rupture strength of the weld joint falls within the scatter band of the base metal at 500 °C, 600 °C and 650 °C [119].

One weld joint made using the Sumitomo welding electrode and the manual metal arc weld-

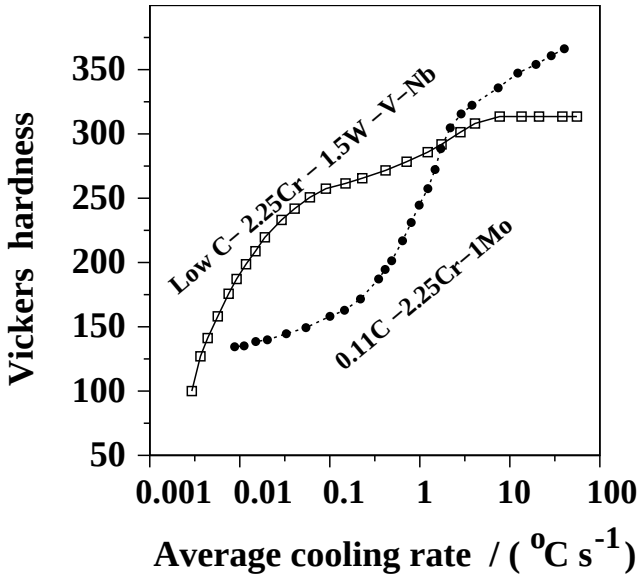

Figure 6.4: Hardness variation in $2\frac{1}{4}$Cr–1Mo and low C–$2\frac{1}{4}$Cr-1.56W-V-Nb steel cooled from the austenitisation temperature. The average cooling rate is that measured in the temperature range 800 °C and 300 °C. The $2\frac{1}{4}$Cr–1Mo steel is austenitised at 950 °C for 0.5 h and low C–$2\frac{1}{4}$Cr-1.56W-V-Nb is at 1050 °C for 0.5 h [121].

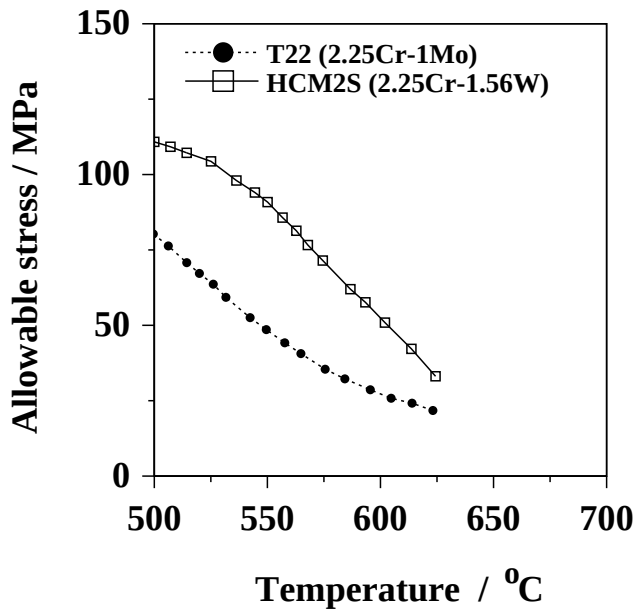

Figure 6.5: The allowable stresses in $2\frac{1}{4}$Cr–1Mo and HCM2S steels at different service temperatures [122].

ing process was provided by National Power, UK. The base plates joined in the process are both $2\frac{1}{4}$Cr–1Mo plates, as shown in Fig. 6.6. The microstructures are as expected, a banded

Process	C	Si	Mn	P	S	Ni	Cr	Mo	W	V	Nb	B	Al
GTAW	0.04	0.50	0.49	0.002	0.005	0.49	2.19	0.10	1.59	0.24	0.033	0.001	0.008
SMAW	0.06	0.41	0.80	0.004	0.002	0.99	2.25	0.10	1.58	0.32	0.040	0.001	—

Table 6.2: Chemical composition (in wt%) of as–deposited weld metal [119].

Process	PWHT	0.2% YS (MPa)	UTS(MPa)	Elongation (%)	Reduction in area (%)
GTAW	As–welded	775	856	20.8	82.2
SMAW	As–welded	877	978	19.8	50.2
SMAW	715 °C × 1h	623	755	21.0	72.0

Table 6.3: Mechanical properties of as–deposited metal [119].

structure in the base plates and a columnar prior austenite grain structure in the weld metal. There is also a clear heat–affected zone. The much more important point is that tests revealed a mean weld metal hardness of 338 HV, with values in the range 306–368 HV. This was considered unacceptable in the context of welding without post–weld heat treatment. Note that the hardness is less than that obtained in the as–welded condition for a $2\frac{1}{4}$Cr–1Mo weld metal (410 HV) but is not low enough to avoid post–weld heat treatment. The task therefore was to design a heat–resistant weld metal having an as–welded hardness less than 300 HV (preferably less than 250 HV).

6.2 Adaptation of Neural Network Weld–Database

A significant difficulty arose during the first attempts at designing the new tungsten–containing weld metal to meet the engineering requirements described above. The problem is illustrated in Fig. 6.7a which was calculated using the input variables described in Table 6.5, and an early version of the neural network model due to Cool *et al.* [27]. The figure shows that the addition of tungsten causes a decrease in the yield strength of the as–deposited weld. This is surprising, since the only role of tungsten in the as–deposited condition is to contribute to solid solution strengthening.

The difficulty arises because the original work [27] was based on a limited weld metal database which included alloys with tungsten, but only for the 9Cr–1Mo type metal. In that system, tungsten promotes the formation of δ–ferrite which weakens the microstructure [123]. The network has learnt this trend and in the absence of knowledge about the influence of tungsten on low–alloy steels, the network simply extrapolates the tungsten influence from the 9Cr–1Mo type alloys to the low–alloy weld metals.

There is, of course, no possibility of δ–ferrite in the final microstructure for the lean alloys considered here. This was verified here using phase diagram calculations [124]. The calculations

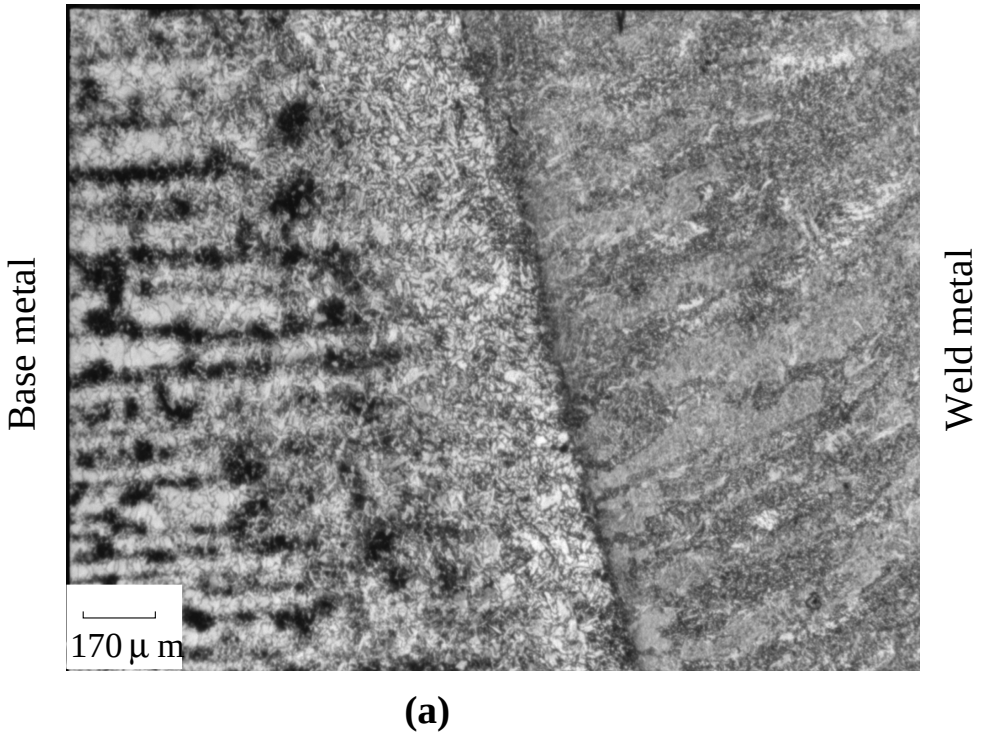

Figure 6.6: $2\frac{1}{4}$Cr-1Mo wt% steel welded using matching HCM2S electrode with manual metal arc welding process. The sample is etched using 2% nital.

show that δ–ferrite does not form in any of the compositions studied. It clearly is necessary to provide the network with knowledge about the role of tungsten in low–alloy steel weld metals. Unfortunately, there are no such data apart from the two welds made by Sumitomo Metal Industries. A procedure was therefore implemented to increase the necessary information in the database, as follows.

In research on fusion reactors, there is an intense effort to develop steels which are resistant to large fluxes of neutrons, particularly in the context of transmutations which lead to radioactive isotopes with large half–lives. There is a search for specific alloys whose radioactivity decays most rapidly once they are removed from the radioactive environment. These are the so–called *reduced activation* alloys which have minimal concentrations of Mo, Ni, Nb, Cu and nitrogen, all of which have long–lived radioactive isotopes [65, 125]. Some of these elements are key constituents of creep–resistant steels, but can be eliminated by using tungsten instead of molybdenum and by substituting vanadium and tantalum for niobium. Some examples of steels which have been studied specifically for their reduced activation are listed in Table 6.4.

There is, therefore, a considerable amount of data on low–alloy tungsten–containing steels in the literature. It was decided to adapt these data and integrate them into the weld metal

Steel	C	Si	Mn	Cr	V	W	Ta	B
$2\frac{1}{4}$Cr–V	0.1			2.25	0.25			
$2\frac{1}{4}$Cr–1WV	0.1			2.25	0.25	1		
$2\frac{1}{4}$Cr–2W	0.1			2.25		2		
$2\frac{1}{4}$Cr–2WV	0.1			2.25	0.25	2		
5Cr–2WV	0.1			5	0.25	2		
9Cr–2WV	0.1			9	0.25	2		
9Cr–2WVTa	0.1			9	0.25	2	0.07	
12Cr–2WV	0.1			12	0.25	2		
$2\frac{1}{4}$Cr–2WVTa	0.1	0.12	0.40	2.41	0.24	2.03	0.05	
$2\frac{1}{4}$Cr–2WVB	0.090	0.12	0.38	2.37	0.24	2.04		0.005
$2\frac{1}{4}$Cr–2WVTaB	0.093	0.12	0.38	2.36	0.24	2.04	0.05	0.005
2.6Cr–2WVTa	0.11	0.11	0.39	2.59	0.25	2.02	0.05	
2.6Cr–2WVTaB	0.11	0.11	0.39	2.60	0.25	2.07	0.05	0.004
$2\frac{1}{4}$Cr–2W	0.11	0.15	0.39	2.48		1.99		
$2\frac{1}{4}$Cr–2WV	0.11	0.20	0.42	2.41	0.24	1.98		
9Cr–2WVTa	0.10	0.23	0.43	8.72	0.23	2.09	0.07	

Table 6.4: Chemical compositions (wt%) of reduced–activation steels, Klueh *et al.* [65]. All of these steels are bainitic with the exception of the 9Cr and 12Cr steels which are martensitic. The chemical compositions of the first group of steels are nominal.

database, by artificially adding a concentration of 300 p.p.m. of oxygen, assuming an interpass temperature of 150 °C, and a heat input of 1.0 kJ mm^{-1}. These modifications all approximately represent average values for the manual metal arc welds. In this way, it was possible to supplement the weld metal database with 34 sets of data on $2\frac{1}{4}$Cr-W-V wrought steels [126, 127, 64]. The new neural network model created using this supplemented database gave trends in the strength of HCM2S which are far more realistic in terms of the trend as a function of the tungsten concentration, Fig. 6.7b.

6.3 Experimental Welds

The wrought $2\frac{1}{4}$Cr–W–V steel data collected from the literature are a minor contribution to the total data set (34 out of 2000). The data add value in the regime of low chromium steels containing tungsten. Nevertheless, the use of plate data to represent welds in the supplemented database left a sense of uncertainty. For this reason, it was decided that it would be useful to measure the mechanical properties of six experimental welds, designed using the neural network based on the supplemented database. The purpose was to see whether the modified network made useful predictions in the regime of interest. In any case, the new experimental data thus generated could be used to create the next generation of neural network models. Using the modified model, six welds were designed with systematic variations in the carbon and tungsten

Input variable	
C (wt%)	0.06
Si (wt%)	0.41
Mn (wt%)	0.87
S (wt%)	0.002
P (wt%)	0.004
Ni (wt%)	0.99
Cr (wt%)	2.01
Mo (wt%)	0.1
V (wt%)	0.27
Cu (wt%)	0.0
Co (wt%)	0.0
W (wt%)	1.52
Ti (wt%)	0.0
B (p.p.m.)	10
Nb (p.p.m.)	400
Heat input (kJ mm^{-1})	1.14
Interpass temperature(°C)	225
Tempering temperature (°C)	715
Tempering time(h)	1

Table 6.5: The input variables of 2.25Cr–1.56W–0.1Mo wt% (HCM2S) steel weld metal used in the analysis of previously developed model.

concentrations, in order to cover a wide range in the $2\frac{1}{4}$Cr–W class of compositions. The variations were around the HCM2S weld metal (Table 6.6).

The set of six experimental manual metal arc welds were made on our behalf and tested by Babcock Welding Products Ltd., UK using a heat input of 1.38 kJ mm^{-1}; the actual chemical compositions are listed in Table 6.7. The results are presented in Table 6.8 and in Fig. 6.8; the experimental data have been predicted to a remarkable degree of accuracy in all three aspects of the tensile test, justifying the use of the plate data within the large weld–database. Given this validation, the new experimental data were themselves incorporated into the plate–supplemented database and a final neural network model was created; this is the one described in detail in Chapter 4, and used in the design of a novel weld deposit for use in industry, as described in the next section.

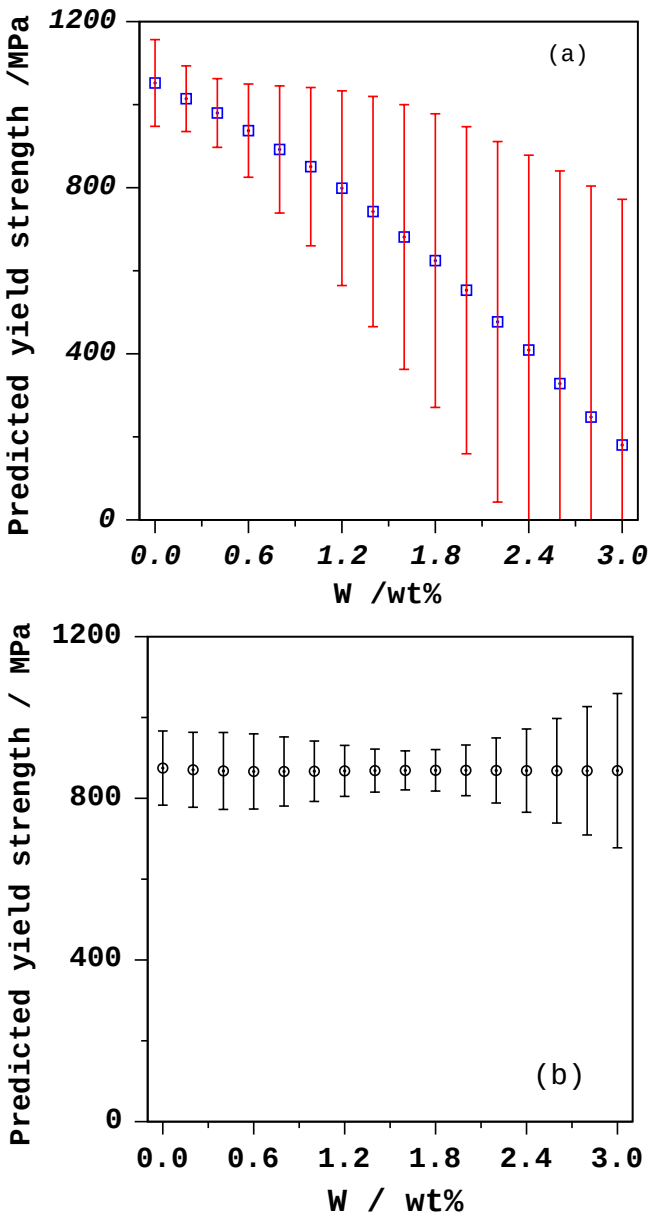

Figure 6.7: The variation in strength in $2\frac{1}{4}$Cr–1.56W–0.1Mo wt% (HCM2S) weld metal in the as–deposited condition, a) using published model [27] b) using the model developed including wrought plate data.

6.4 Theoretical Design of New Weld Metal

The main task was to design a heat–resistant weld metal with hardness consistently lower than 300 HV. Since the neural network model predicts strength rather than hardness, it is necessary to convert between these two variables. The hardness can be estimated as a function of the yield

Variable	Weld 1	Weld 2	Weld 3	Weld 4	Weld 5	Weld 6
C (wt%)	0.06	0.06	0.06	0.10	0.10	0.10
Si (wt%)	0.3–0.4	0.3–0.4	0.3–0.4	0.3–0.4	0.3–0.4	0.3–0.4
Mn (wt%)	0.6	0.6	0.6	0.6	0.6	0.6
S (wt%)	0.005–0.01	0.005–0.01	0.005–0.01	0.005–0.01	0.005–0.01	0.005–0.01
P (wt%)	0.005–0.01	0.005–0.01	0.005–0.01	0.005–0.01	0.005–0.01	0.005–0.01
Cr (wt%)	2.1–2.4	2.1–2.4	2.1–2.4	2.1–2.4	2.1–2.4	2.1–2.4
Mo(wt%)	≤ 0.1	≤ 0.1	≤ 0.1	≤ 0.1	≤ 0.1	≤ 0.1
Ni (wt%)	1.0	1.0	1.0	1.0	1.0	1.0
B (p.p.m.)	10	10	10	10	10	10
O (p.p.m.)	300	300	300	300	300	300
N (p.p.m.)	80	80	80	80	80	80
Nb (p.p.m.)	400	400	400	400	400	400
V (wt%)	0.25	0.25	0.25	0.25	0.25	0.25
W(wt%)	0.5	1.0	1.5	0.5	1.0	1.5

Table 6.6: The designed weld metals with variations in carbon and tungsten.

Variable	Weld 1	Weld 2	Weld 3	Weld 4	Weld 5	Weld 6
C (wt%)	0.053	0.059	0.059	0.11	0.10	0.10
Si (wt%)	0.27	0.32	0.34	0.40	0.39	0.4
Mn (wt%)	0.6	0.68	0.7	0.72	0.72	0.76
S (wt%)	0.007	0.007	0.006	0.006	0.006	0.007
P (wt%)	0.010	0.012	0.012	0.012	0.012	0.012
Cr (wt%)	2.22	2.22	2.29	2.26	2.31	2.35
Mo (wt%)	0.04	0.04	0.04	0.04	0.04	0.04
Ni (wt%)	0.99	0.97	1.03	0.98	0.99	0.99
B (p.p.m.)	≤ 10	≤ 10	≤ 10	≤ 10	≤ 10	≤ 10
O (p.p.m.)	550	550	550	550	550	550
N (p.p.m.)	180	160	130	130	130	140
Nb (p.p.m.)	300	400	400	500	500	500
V(wt%)	0.20	0.22	0.23	0.23	0.23	0.24
W (wt%)	0.5	1.01	1.48	0.5	1.02	1.54

Table 6.7: Experimental weld metals made with heat input 1.38 kJ mm^{-1} and interpass temperature of 300–350 °C.

strength as follows [128]:

$$\text{Yield strength} \cong \frac{\text{Vickers Hardness}}{3} \times 9.81 \qquad \text{(MPa)} \tag{6.1}$$

The base composition for the new weld metal is similar to that of HCM2S steel but with certain key modifications, Table 6.2. To avoid excessive hardness in the as–welded condition, the carbon concentration has been restricted to a maximum of 0.05 wt%. HCM2S steel contains

Property	Predicted Weld 1	Measured Weld 1	Predicted Weld 2	Measured Weld 2
YS (MPa)	796 ± 88	705	838± 77	842
UTS (MPa)	851 ± 79	844	905 ± 76	899
Elongation (%)	20 ± 8	19	21 ± 8	21
	Weld 3	**Weld 3**	**Weld 4**	**Weld 4**
YS(MPa)	853 ± 57	804	891 ± 105	893
UTS (MPa)	930 ±64	924	1001 ± 148	1048
Elongation (%)	30 ± 11	30	22± 9	22
	Weld 5	**Weld 5**	**Weld 6**	**Weld 6**
YS (MPa)	895 ± 95	828	913 ± 72	922
UTS (MPa)	1006 ± 136	1085	1031 ± 135	1155
Elongation(%)	21 ± 9	21	21 ± 11	21

Table 6.8: The predicted and measured values for the experimental as-welded metals.

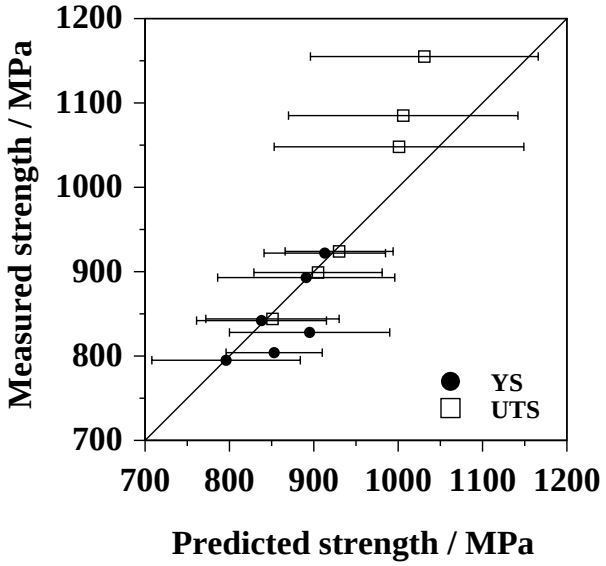

Figure 6.8: Comparison between predicted and measured strengths of designed experimental welds. The error bars represent the predicted range.

400 p.p.m. of niobium, but the literature [129, 29] suggests that niobium is harmful in the context of low–alloy steel welds because it leads to a deterioration in the toughness. A number of mechanisms have been proposed for the effect of niobium; for example, it may cause precipitation hardening, increase the yield strength and hence reduce the toughness. However, there are quite contradictory reports on its influence on microstructure, particularly in altering the balance between acicular ferrite and bainite. None of these effects are well–established, but the experimental evidence regarding toughness is clear. Therefore, it was decided to avoid niobium altogether. It will be seen later that MX type precipitates probably contribute to the creep

strength of HCM2S, but the steel also contains a larger fraction of vanadium carbonitrides. The omission of niobium was therefore judged not to be of critical importance in the design of the weld metal. It turned out in practice that it was not possible to completely avoid niobium because of the commercial purity raw materials used for the welding consumable manufactured as a consequence of the work presented in this Chapter.

Vanadium in steels forms stable V_4C_3 carbides which are beneficial in the context of creep; vanadium is therefore a key element in the proposed weld metal.

Recent work has suggested that a reduction in the manganese concentration can lead to an improvement in creep strength [120]. A reduction in the manganese concentration in HCM2S slows down M_6C precipitation, which contains tungsten as the major metallic element. Thus, a lower manganese concentration allows tungsten to remain dissolved in ferrite and strengthen the solid solution. However, in shielded metal arc welding, around 0.6 wt% manganese is essential as a deoxidising element and to ensure good weldability. In manual metal arc welding, manganese and silicon assist the formation of a fluid slag at low melting temperature, thus preventing slag inclusions in the weld metal. Boron is beneficial in increasing the creep life [120]. It stabilises $M_{23}(C,B)_6$ precipitates along grain boundaries, thereby preventing the recrystallisation of grains during service at high temperatures. However, it is also a difficult element to control during its transfer across the welding arc; the weld metal design therefore does not rely on boron which is set at a trace concentration of 10 p.p.m. The ideal composition that emerged after careful analysis of the role of each of the chemical constituents using the final neural network models described in detail in Chapter 3, and in the light of experience from physical metallurgy, is given in Table 6.9. The table also includes a set of tolerances which were arrived at by discussion with manufacturing industry.

The error bars presented in Table 6.9, however, refer to the mean composition only. It must be emphasised that the error bars consist of two components (Chapter 3), one describing the perceived level of experimental noise ($\sigma_\nu \simeq \pm 0.048$), and the other reflecting the uncertainty in fitting a function within a local region of the input space. This latter error will necessarily be large when dealing with novel alloys not available at the time of the creation of the neural network model. The magnitude of this fitting error gives a warning that the model is being used in extrapolation or in a region where there is a lack of knowledge, but the mean prediction may nevertheless be reliable if the proper functional form has been recognised in the region covered by data. The hardness values were calculated using equation 6.1.

6.4.1 Creep Rupture Strength

Cole *et al.* [130] have developed a comprehensive neural network model which permits the estimation of the creep rupture strength of ferritic steels as a function of the detailed chemical

Input variable	
C (wt%)	0.05 ± 0.02
Si (wt%)	0.30 ± 0.15
Mn (wt%)	0.70 ± 0.15
S (wt%)	0.007
P (wt%)	0.010
Ni (wt%)	≤ 0.05
Cr (wt%)	2.22 ± 0.2
Mo (wt%)	0.20 ± 0.1
V (wt%)	0.20 ± 0.005
Cu (wt%)	0.03
Co (wt%)	0.0
W (wt%)	0.6 ± 0.1
O (p.p.m.)	300
Ti (wt%)	250 ± 50
B (p.p.m.)	10 ± 5
Nb (p.p.m.)	50 ± 10
Heat input (kJ mm^{-1})	1.38
Interpass temperature (°C)	300
Tempering temperature (°C)	20
Tempering time (h)	0
Estimated YS (MPa)	714 ± 216
Estimated UTS (MPa)	851 ± 112
Estimated elongation (%)	19 ± 15
Estimated Vickers hardness	225

Table 6.9: The designed input variables of 2.25Cr–0.56W–0.2Mo wt% (HCM2S) as–welded metal.

composition and a set of up to three separate heat treatments. Furthermore, it has been demonstrated that by assuming a selected austenitisation heat treatment, the model can be used to estimate the creep rupture life of weld deposits even though the neural network has no prior knowledge of welds.

It would obviously be useful to be able to estimate the creep rupture life of the new weld described in Table 6.9. However, Cole's model suffers from the same problem as encountered here, that there are virtually no data on the creep of low chromium, tungsten–containing steels. There are plenty of data on 9Cr–1Mo type alloys with tungsten, but the metallurgy of tungsten in those alloys is different for the reasons described previously. In view of the lack of low–Cr data, it would be useful to study the behaviour of the Cole model with respect to four experimental

data that exist for the Sumitomo Metal Industries welding alloys described in [119]. Fig. 6.9a shows that the actual creep rupture stress is greatly overestimated; that this is due to the lack of appropriate knowledge in the Cole model can be proved by repeating the calculation whilst setting the tungsten concentration to zero, as illustrated in Fig. 6.9b, which shows that the experimental data are well–predicted. The importance of the latter result is that it should be possible to estimate the creep rupture life of the proposed new weld (Table 6.9), simply by ignoring the fact that it contains a small concentration of tungsten. The results are illustrated in Fig. 6.10, which shows that the long–term creep rupture strength of the new welding alloy should be comparable to that of HCM2S tube.

6.5 New Welding Alloy: Experimental Results

The new welding alloy was manufactured by Mitsui Babcock Welding Products Ltd., UK and Table 6.10 shows a comparison between what was proposed and what was achieved in practice. The table also shows that the theoretical design procedure has been very successful in predicting the mechanical properties; the electrode is now marketed with the commercial designation BWPL (Babcock Welding Products Ltd.) J–type electrode. It is intended to market this both for power plant boiler components and for other applications where welding can be conducted without the need for post–weld heat treatment. Microstructural studies of the new alloy will be described in Chapter 7.

6.6 Conclusions

The series of neural network models created in this work have been used, along with metallurgical experience, to create a new welding alloy which is now available on a commercial scale. The entire design process, including the creation of the models, took less than two years and was successful at the first attempt. The models can now be used to develop new electrodes over much shorter time scales. There are also some lessons learnt about the neural network method, in particular how the database can be "manipulated" for specific purposes. The models themselves can be manipulated to reduce uncertainties, as illustrated with the estimation of creep rupture life for the new alloy. The design example presented here is but one of the success stories of the present work – some other examples are listed in Appendix B.

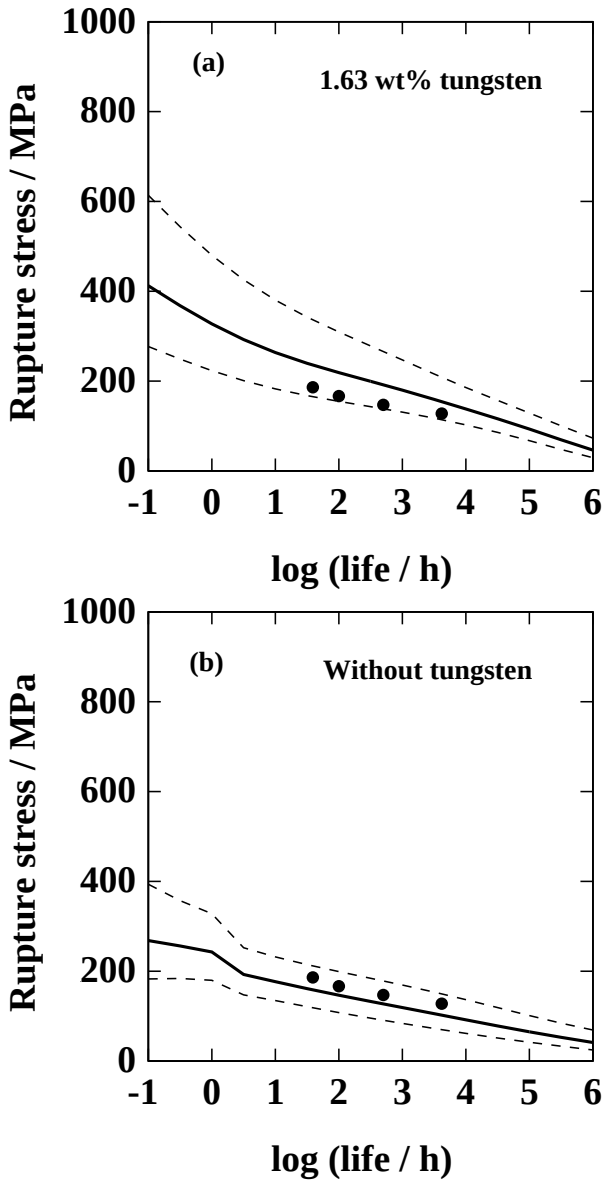

Figure 6.9: Effect of tungsten on the calculated creep strength of 0.062C–0.1Mn–2.27Cr–0.026V–0.05Nb wt% weld metal, using a published model [130]. The measured points are for 1.63 wt% tungsten from literature [120].

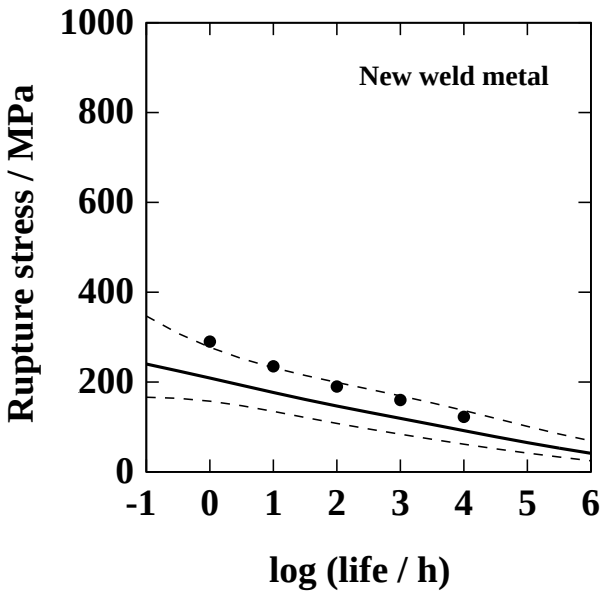

Figure 6.10: Calculated creep strength of designed weld metal (with 0.1 wt% manganese) using a published neural network model [130]. The points are for HCM2S steel tube creep data are extracted from published literature [131].

Input variable	**Proposed**	**Actual**
C (wt%)	0.05 ± 0.02	0.057
Si (wt%)	0.30 ± 0.15	0.32
Mn (wt%)	0.70 ± 0.15	0.67
S (wt%)	0.007	0.005
P (wt%)	0.010	0.009
Ni (wt%)	≤ 0.05	0.07
Cr (wt%)	2.22 ± 0.2	2.10
Mo (wt%)	0.20 ± 0.1	0.20
V (wt%)	0.20 ± 0.005	0.20
Cu (wt%)	0.03	≤ 0.02
Co (wt%)	0.0	0.0
W (wt%)	0.6 ± 0.1	0.63
O (p.p.m.)	300	≤ 0.02
Ti (wt%)	250 ± 50	≤ 200
B (p.p.m.)	10 ± 5	≤ 20
Nb (p.p.m.)	50 ± 10	≤ 200
Heat input(kJ mm^{-1})	1.38	1.35
Interpass temperature ($^{\circ}$C)	300	350 (max.)
Tempering temperature ($^{\circ}$C)	20	**as–welded**
Tempering time (h)	0	-
YS (MPa)	714 ± 216	678
UTS(MPa)	851 ± 112	774
Elongation(%)	19 ± 15	19.5
Vickers hardness	225	228

Table 6.10: Comparison between the proposed and experimental results of new weld metal.